Macalester Journal of Physics and Astronomy

Volume 8
Issue 1 *Spring 2020*

Article 6

May 2020

Modeling Scavenging for a Hydraulic Free-Piston Engine

Nathan Davies
Macalester College, ndavies1@macalester.edu

Modeling Scavenging for a Hydraulic Free-Piston Engine

Abstract

The hydraulic free-piston engine at the University of Minnesota offers a solution to improve the hydraulic efficiency and reduce emission output of off-road vehicles. We developed a MATLAB Simulink model to track the pressure, temperature, and mass profile of the fuel within the cylinder during operation. By varying different initial conditions of our model, we found that a higher intake manifold pressure and larger bottom dead center location results in higher scavenging efficiency. These results can be used to improve the controller of this engine and better maintain stable operation.

Keywords

Scavenging Hydraulic Free-Piston Engine

Cover Page Footnote

I would like to thank the Center for Compact and Efficient Fluid Power at the University of Minnesota for providing me with this research experience. I would also like to thank Dr. Zongxuan Sun and Dr. Chen Zhang for their guidance on this project and Ford Motor Company for their generous donation of the hydraulic free-piston engine.

Modeling Scavenging for a Hydraulic Free-Piston Engine

Nathan Davies

Department of Physics & Astronomy,

Macalester College, St Paul, MN 55105

(Dated: February 19, 2020)

Abstract

The hydraulic free-piston engine at the University of Minnesota offers a solution to improve the hydraulic efficiency and reduce emission output of off-road vehicles. We developed a MATLAB Simulink model to track the pressure, temperature, and mass profile of the fuel within the cylinder during operation. By varying different initial conditions of our model, we found that a higher intake manifold pressure and larger bottom dead center location results in higher scavenging efficiency. These results can be used to improve the controller of this engine and better maintain stable operation.

CONTENTS

I. INTRODUCTION

A. Hydraulics overview

The National Fluid Power Association defines hydraulics as technology that uses fluid to transmit power from one location to another.[4] Hydraulics often uses rotational power from an electric or gas motor then transmits it into linear motion by pumping hydraulic fluid into and out of a hydraulic actuator. It can also transmit the rotational power to another location by spinning a hydraulic pump.

The main advantage of hydraulics over other means of power conversion is its high power density. Hydraulic systems require much smaller components than mechanical or electrical drives for use in high force or high torque applications.[4] Hydraulic technology is used for large off-road vehicles, such as excavators, farm equipment, and logging vehicles. Improving the efficiency of these off-road vehicles is important in order to lower emissions, environmental impacts, and economic costs.

B. Free-piston engine overview

In a traditional internal combustion engine (ICE), the energy from igniting the fuel pushes a piston downwards that uses a series of mechanical linkages and cams in order to spin a crankshaft. The energy created by ignition is converted into mechanical power which can then be converted into electrical or hydraulic power with a generator or pump. Free-piston engines have crank-less designs and use the linear motion of the piston to create electrical or hydraulic power directly. Linear free-piston generators (LFPG) create electrical power by moving a magnet back and forth through a coil. Hydraulic free-piston engines (HFPE) create hydraulic power by pushing hydraulic fluid through chambers under high pressure. LFPGs and HFPEs have many advantages over ICEs as they require fewer components to generate electrical or hydraulic power, are easier to maintain, and have adjustable operating parameters, such as compression ratio, since they do not have fixed mechanical linkages.

II. HYDRAULIC FREE-PISTON ENGINE AT UNIVERSITY OF MINNESOTA

A. Engine architecture and design

The HFPE at the University of Minnesota was originally developed by Ford Motor Company for use in their F-150 truck before being donated to the University. This engine combines the engine and pump to generate fluid power directly instead of having two separate units. This engine-pump design will increase efficiency and decrease the emissions of off-road vehicles. It is a two-stroke opposed-piston opposed-cylinder (OPOC) internal combustion engine. This design enables the HFPE to have the highest power density and scavenging among FPE architectures. Further, it has a variable compression ratio which allows for multi-fuel operation as well as the implementation of homogeneous charge compression ignition (HCCI), the auto-ignition of fuel from compression alone.[2]

A schematic of this engine in shown in Fig. 1. In this diagram, the right chamber is at top dead center (TDC), where the cylinder is most compressed and the ideal location for ignition to occur, and the left chamber is at bottom dead center (BDC), when the cylinder is least compressed. Starting with this situation, after ignition occurs in the right cylinder, the force would push the inner piston pair to the left and the outer piston pair to the right, compressing the left cylinder until its TDC is reached and opening the right cylinder until its BDC. Then, ignition occurs in the left cylinder, pushing the inner piston pair back to the right and the outer piston pair to left until the engine returns to its position in Fig. 1 and completing its cycle.

During its operation, the HFPE pumps hydraulic fluid into either a high or low pressure accumulator.[2] These accumulators act similarly to capacitors in electronics. Inside the tanks there is a helium gas balloon. When fluid is pumped into the accumulator, it compresses the helium balloon and holds the fluid under pressure, storing energy. This fluid can then be released at a later time to use the stored energy. These accumulators allow the engine to have a variable compression ratio and also are key for maintaining stable operation of the engine.

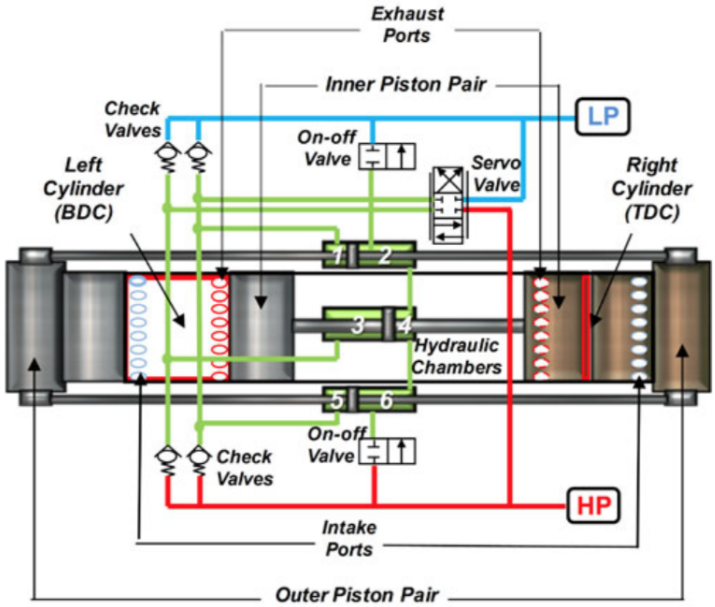

FIG. 1. A schematic of the HFPE at the University of Minnesota.[2] In this image, the right cylinder is at its TDC and the left cylinder is at its BDC. When ignition occurs, the force from combustion will push the inner piston pair to the left and the outer piston pair to the right. This prcoess will compress the left cylinder to its TDC and open the right cylinder to its BDC. During operation, hydraulic fluid is pumped into either the high or low pressure accumulator.

Engine specifications and parameter values can be found in Tables I and II. We used these values to design our model for this specific free-piston engine.

Item	Specification
Bore	79.5 mm
Maximum stroke/Piston	65 mm
Displacement/Cylinder	0.6 L
Inner plunger diameter	13.4 mm
Outer plunger diameter	9.5 mm
Piston mass	9 kg

TABLE I. A table of specifications of different components for the HFPE.[2]

Symbol	Definition	Value
γ	Specific heat ratio	1.31
R	Gas constant	296.25 J/Kg K
C_d	Discharge coefficient	0.6
P_{int}	Intake manifold pressure	1.5 bar
T_{int}	Intake manifold temperature	350 K
x_{int}	Intake port location	50 mm
A_{int}	Intake port area	2000 mm^2
P_{ex}	Exhaust manifold pressure	1 bar
T_{ex}	Exhaust manifold temperature	500 K
x_{ex}	Exhaust port location	50 mm
A_{ex}	Exhaust port area	2200 mm^2

TABLE II. A table of different values and constant definitions for the HFPE used in our model.[2]

B. Control challenges

In a crankshaft-based ICE, the crankshaft is the controlling mechanism of piston trajectory. The spinning crankshaft controls the timing of each cylinder and its angular momentum allows for piston trajectory to be maintained if a misfire occurs. For a FPE, if a misfire occurs, there will not be enough force to compress the cylinder the required amount on the next cycle. Therefore, in order to maintain stable operation a new control mechanism must be developed.

The solution that Dr. Zongxuan Sun and his team is developing is an active piston motion controller which acts as a virtual crankshaft for the engine.[2] The virtual crankshaft uses the energy stored within the accumulators to regulate the pistons to a predefined trajectory. For this HFPE, when a misfire occurs in a cylinder, the accumulators would release some of its stored energy to compensate for the lack of force, and provide the necessary compression for a proper ignition on the next cycle. The goal of this paper is to better understand the engine's dynamics under operation to improve this controller and see which parameters influence scavenging efficiency.

C. Scavenging

For an ICE, scavenging is the process in which exhaust fuel exits the cylinder and fresh fuel enters the cylinder for combustion on the next cycle. In a two-stroke engine, the exhaust fuel exits out the exhaust port and fresh fuel enters in through the intake simultaneously, during the same cylinder stroke. In a four-stroke engine, the removal of the exhaust fuel and input of fresh fuel occur on independent, designated strokes. We define scavenging efficiency as

$$scav_{eff} = \frac{m_{curr}}{m_{prev}}$$

where m_{prev} is the mass within the cylinder during compression of the previous cycle and m_{curr} is the mass within the cylinder during the current cycle.

For the HFPE at the University of Minnesota, the exhaust ports are located near the inner piston pair while the intake ports are near the outer piston pair. When cylinders expand towards BDC after combustion, they uncover the exhaust and intake ports simultaneously in order to replace the exhaust fuel with fresh charge. Since the ports are located on opposite sides of the cylinder, this allows for uniflow scavenging, where the fresh fuel moves in the same direction as the exhaust flows out. In order to more accurately compute the gas mixing outcome, Benson's model is applied, which divides scavenging into a two-zone, two-stage process.[1] A diagram of Benson's model is shown in Fig. 2 below. During the first stage of this process, fresh charge enters the cylinder and mixes with the residual gas to form a mixture of each, while residual gas also leaves out the exhaust port. Then after a short time and if the ports remain open for a long enough time, some of this fresh-residual gas mixture begins exiting out the exhaust port. The model is based on the following assumptions:[3]

- There is uniform pressure across the chamber.
- Temperature in each zone is uniform and two zones can have distinct temperature.
- There is no heat transfer between zones.
- Molecular weight and specific heat of the gas are identical.

Using this model, along with specifications specific to the HFPE at the University of Minnesota, we developed another model to track the pressure, temperature, and mass profile of one engine cylinder during operation.

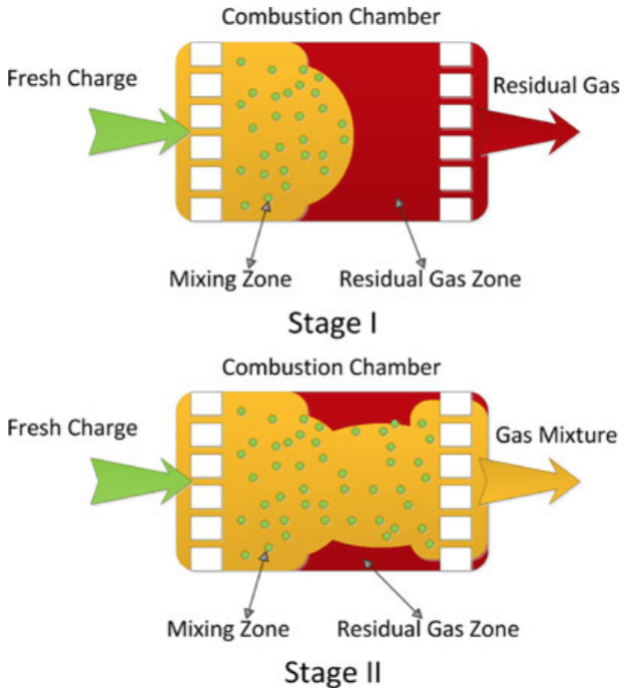

FIG. 2. A figure of Benson's model applied for scavenging for the HFPE.[2]

III. MATLAB SIMULINK MODEL

We used MATLAB Simulink to build a scavenging model for the hydraulic free-piston engine at the University of Minnesota. The goal of our model was to track the mass, temperature, and mass profile of fuel within one cylinder and calculate its scavenging efficiency. First, we inputted a single period sine wave to simulate the piston motion for one cycle. We fit this sine wave according to the parameters in Tables I and II to match operating conditions of the engine.[2] Shown below in Fig. 3, our sine wave had a stroke length of 60 mm, a BDC of 62.5 mm, a TDC of 2.5 mm, and operated at 25 Hz, 1500 cycles per minute.

The green line represents the locations of the intake and the exhaust ports. When the blue curve is below the green line, the ports are closed and fuel does not flow into or out of the cylinder. When the blue curve is above the green line, the ports are open and new fuel flows in to replace the exhaust that flows out of the cylinder. We set the cycle of our model to start and end at the instance when the ports close. Each situation, ports open and ports closed, have a system of equations that describe the mass, temperature, and pressure profile of the fuel in the cylinder during operation.

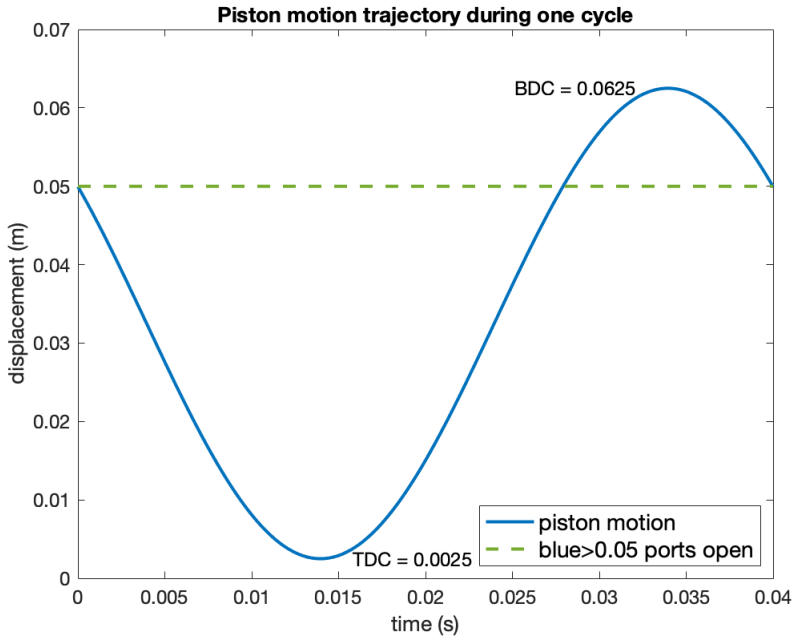

FIG. 3. A graph of piston trajectory used during simulations. The blue curve, a sine wave, is used with a BDC of 0.0625 m and a TDC of 0.0025 m. The green line represents the locations of intake and exhaust ports. When the blue curve is below the green line, the ports are closed and no fuel is transferred through the cylinder. When the curve is above the green line, the ports are open and fuel flows into and out of the cylinder. The cycle starts and ends at the instance the ports close.

A. Equations for when ports closed

When the ports are closed the fuel inside the cylinder is a closed system. Therefore, we set the initial cylinder pressure and temperature to be equal to the intake manifold pressure and temperature. We assume that the fuel within the cylinder is an ideal gas and calculate the initial mass within the system using the ideal gas law

$$PV = mRT$$

rewritten so

$$m_i = \frac{P_o V_o}{R T_o} \tag{1}$$

where m_i is the initial mass of fuel in the cylinder in kg, P_o is pressure in Pa, V_o is volume in m^3, R is the gas constant, and T_o is temperature in K at time t_o, when the ports first close. For our model, we used intake manifold pressure as P_o and intake manifold temperature as

T_o. Volume within the cylinder is calculated taking the displacement of the piston from 0 multiplied by the bore of the engine.

We make a further assumption that the system is an ideal gas undergoing an adiabatic process, that there is no heat transfer into the walls of the cylinder from the fuel. To represent this system, we can use the polytropic process equation

$$PV^{\gamma} = C$$

where P is pressure, V is volume, and γ is the specific heat ratio. With the ports closed, we can use this equation to find the pressure, and subsequently the temperature, at every time step since the constant remains the same if no energy is added to the system. First we have the pressure and volume given at t_o, when the ports first close

$$P_o V_o^{\gamma} = C$$

and also at a later time step

$$P_j V_j^{\gamma} = C$$

We can then set the left sides of these equations equal to one another and solve for P_j

$$P_j = \frac{P_o V_o^{\gamma}}{V_j^{\gamma}} \tag{2}$$

However, Eq. 2 does not incorporate combustion which occurs when the piston reaches its TDC. When combustion occurs, the fuel in the cylinder ignites, adding energy into the system and spiking the temperature of the fuel. To include combustion, we calculated what the pressure and temperature would be when the piston reaches its TDC, then added the increase of temperature from the ignited gas to get T_{TDC}, the temperature at TDC.[5] We used the ideal gas law solved for pressure at TDC

$$P_{TDC} = \frac{m_i R T_{TDC}}{V_{TDC}}$$

Then, we used this P_{TDC} similar to as in Eq. 2, to solve for the pressure in the cylinder after combustion with the ports closed

$$P_j = \frac{P_{TDC} V_{TDC}^{\gamma}}{V_j^{\gamma}} \tag{3}$$

At each time step, using the results from either Eq. 2 or 3, we can solve for the temperature at step j by solving the ideal gas law for T

$$T_j = \frac{P_j V_j}{m_i R} \tag{4}$$

Using Eq. 1, 2, 3, and 4 we can track the mass, pressure, and temperature profile of the fuel within the cylinder during operation when the ports are closed. Our model makes assumptions to avoid the molecular dynamics of the fuel that occur during compression and combustion. We are also assuming ideal piston trajectory by using a sine wave. These assumptions have been made to simplify the model to fit the scope of this project while also providing an accurate representation of the dynamics of the system.

B. Equations for scavenging

When the ports are open, during the portion of Fig. 3 where the blue curve is above the green line, scavenging occurs. When the ports open, fuel flows out the exhaust port since cylinder pressure is much greater than the exhaust manifold pressure. Fresh charge then begins flowing into the cylinder once the cylinder pressure is lower than the intake manifold pressure. Mass flow through an orifice, or port, is a complex equation to solve; thus, for mass flow in and out of the cylinder, we used equations previously defined by Ke Li, Ali Sadighi, and Zongxuan Sun.[2] For choked flow, when $P_T/P_o \leq (2/(\gamma+1))^{\gamma/(\gamma-1)}$, we used

$$\dot{m} = \frac{C_d A_R P_o}{\sqrt{RT_o}} \sqrt{\gamma} \left(\frac{2}{\gamma+1}\right)^{\frac{\gamma+1}{2(\gamma-1)}} \tag{5}$$

For subsonic flow, when $P_T/P_o > (2/(\gamma+1))^{\gamma/(\gamma-1)}$, we used

$$\dot{m} = \frac{C_d A_R P_o}{\sqrt{RT_o}} \left(\frac{P_T}{P_o}\right)^{1/\gamma} \sqrt{\frac{2\gamma}{\gamma-1}\left(1 - \left(\frac{P_T}{P_o}\right)^{\frac{\gamma-1}{\gamma}}\right)} \tag{6}$$

where C_d is the discharge coefficient, P_T is the pressure downstream, A_R is the port opening area, and P_o and T_o are the upstream pressure and temperature. An important takeaway from these equations is the dependence, or lack thereof, on the ratio of downstream pressure divided by upstream pressure. If the difference in pressure between up and downstream is large enough, we are in a state of choked flow, the maximum rate in which fluid can flow through a port. In subsonic flow, mass flow rate will vary depending on the difference in

pressure between the chambers on either side of the port and be below the maximum possible rate. For each time step in our model, we used the mass, pressure, and temperature profile from the previous step to determine how much residual fuel left through the exhaust port and how much new fuel entered through the intake.

To calculate temperature within the cylinder at each time step, we found the average of temperature of new fuel and residual fuel within the cylinder using

$$T_j = \frac{m_{res}T_{j-1} + m_{int}T_{int}}{m_{res} + m_{int}} \tag{7}$$

where T_{j-1} is the temperature within the cylinder during the previous step, T_{int} is the temperate of the intake fuel, m_{res} is the mass of the residual fuel remaining within the cylinder, and m_{int} is the mass of the new fuel from the intake.

Lastly, to calculate the pressure within the cylinder during scavenging, we used the ideal gas law so

$$P_j = \frac{T_j(m_{res} + m_{int})R}{V_j} \tag{8}$$

Using Eq. 5, 6, 7, and 8 we can track the mass, pressure, and temperature profile of the fuel within the cylinder during operation when the ports are open and scavenging is occurring.

C. Changing model parameters

To run our model, we used the specifications and parameters outlined in Tables I and II and the equations outlined above. We analyzed the effects of varying four different parameters, intake manifold pressure, intake manifold temperature, air-fuel ratio, and BDC location, while holding all others constant. This process allowed us to examine how each of these parameters impacted scavenging efficiency.

IV. RESULTS AND DISCUSSION

Our model showed that varying intake manifold temperature and air-fuel ratio did not have a significant impact on the scavenging efficiency of the engine. For intake manifold temperature, we varied it from 300-500 K and found the total difference in scavenging efficiency to be less that 0.3%. For air-fuel ratio, we varied the ratio from 1:1 to 3.4:1 and this had an insignificant impact on scavenging as the difference was less than 0.1%.

A. Varying intake manifold pressure

Varying intake manifold pressure had the greatest impact on scavenging efficiency. We varied intake pressure from $1.5 * 10^5$ to $2.5 * 10^5$ Pa in steps of 10^4 Pa. Plots of the pressure, temperature, and mass profiles for these runs, along with a plot of scavenging efficiency, can be found in Fig. 4, 5, 6, and 7 respectively.

For pressure within the cylinder, all the runs follow a similar profile: increasing initially as the gas is compressed, spiking when combustion occurs, decreasing as the volume within the cylinder expands, and then dropping again once the intake and exhaust ports open. As intake pressure increases, each subsequent run has a slightly larger initial mass due to our definition of m_i in Eq. 1 being dependent on intake manifold pressure. This increase in mass subsequently causes the pressure in the cylinder to be larger as well.

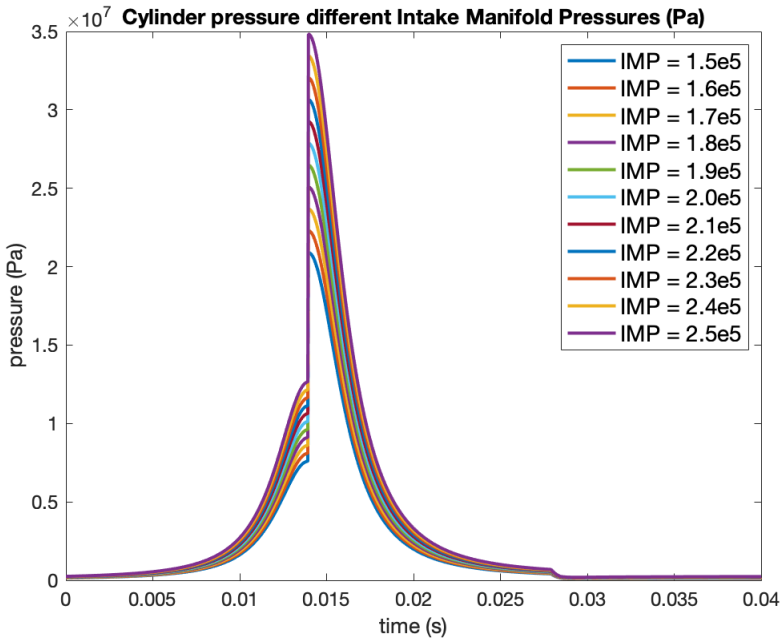

FIG. 4. Cylinder pressure results for varying intake manifold pressure. As the cylinder compresses the fuel, pressure increases until before spiking at combustion due to a rapid increase of temperature. Then pressure decreases as the cylinder volume expands before dropping again when the intake and exhaust ports open.

In Fig. 5, temperature within the cylinder was nearly identical for all the runs of varying intake pressure. First, the temperature increases as pressure increases, then spikes when the

fuel ignites, before decreasing as pressure decreases, and then dropping as the hot exhaust exits the cylinder and new fresh fuel enters. Although pressure increases between runs due to m_i increasing, this effect is canceled out for temperature by the division of m_i in Eq. 4. When combustion occurs, again, the difference in mass is canceled out when accounting for the spike in temperature.[5] The difference in temperature between runs occurs only during scavenging once the ports open.

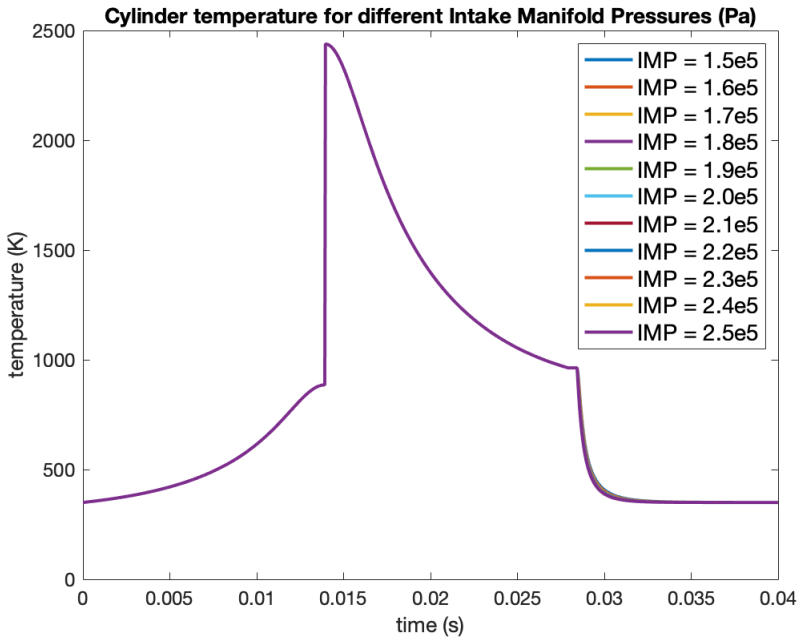

FIG. 5. Temperature results for varying intake manifold pressures. Temperature rises as cylinder volume decreases, then spikes when combustion occurs, before decreasing as the cylinder volume expands. When the ports open, the temperature drops to the temperature of the fuel entering through the intake manifold.

In Fig. 6, the time axis varies from 0.02 to 0.04 seconds to focus on the portion of our model when the ports are open. Mass is constant before the ports open to let exhaust out and new fuel in. Once the ports open initially, the hot exhaust gas leaves through the exhaust port much quicker than fresh fuel enters through the intake, causing mass within the cylinder to drop. Then the opposite occurs as intake fuel enters quicker than fuel out of the exhaust port, causing mass to rise to a maximum. At this point, the mass entering through the intake is equal to the mass leaving out the exhaust port and occurs close to the BDC of the piston. As the volume of the cylinder begins shrinking after BDC, the mass within

the cylinder decreases until the ports close again. For smaller intake manifold pressures, the mass within the cylinder never increases much above its initial value; on the contrary, at higher intake manifold pressures, the mass within the cylinder becomes significantly larger than its initial value before decreasing.

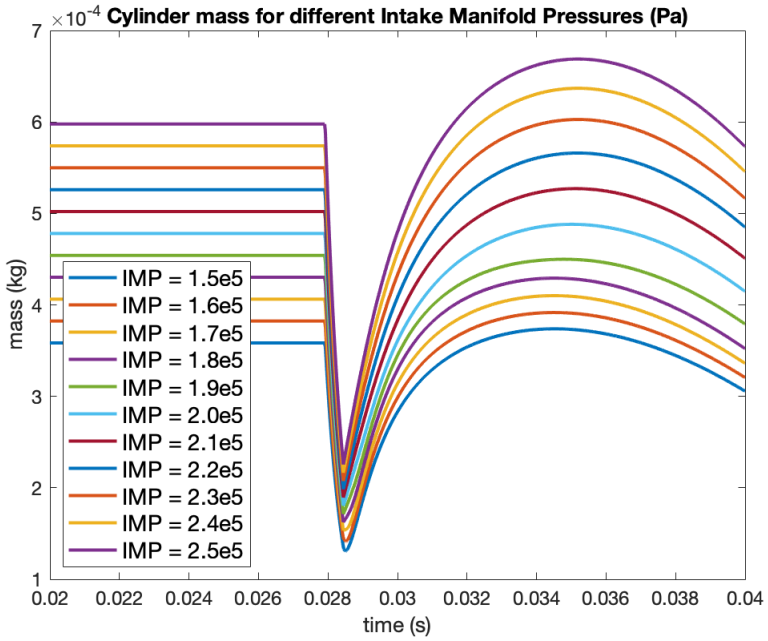

FIG. 6. Cylinder mass results for varying intake manifold pressure. Once the ports open, the exhaust fuel leaves quickly out of the exhaust port and fresh fuel begins entering through the intake port. The mass in the cylinder reaches a maximum near the time of the cylinder reaching BDC.

In Fig. 7, scavenging efficiency initially goes down by about 3% as intake pressure increases from 1.5 to $1.8 * 10^5$ Pa. From 1.8 to $2.5 * 10^5$ Pa, scavenging efficiency increases from 82% to 96%. At higher intake manifold pressures, there is a greater pressure difference across the intake port which results in fresh fuel flowing in at the choked flow rate for longer periods of time. Essentially, there is more force pushing fresh fuel into the cylinder of the engine, resulting in more fuel being in the cylinder at the end of the cycle which increase scavenging efficiency.

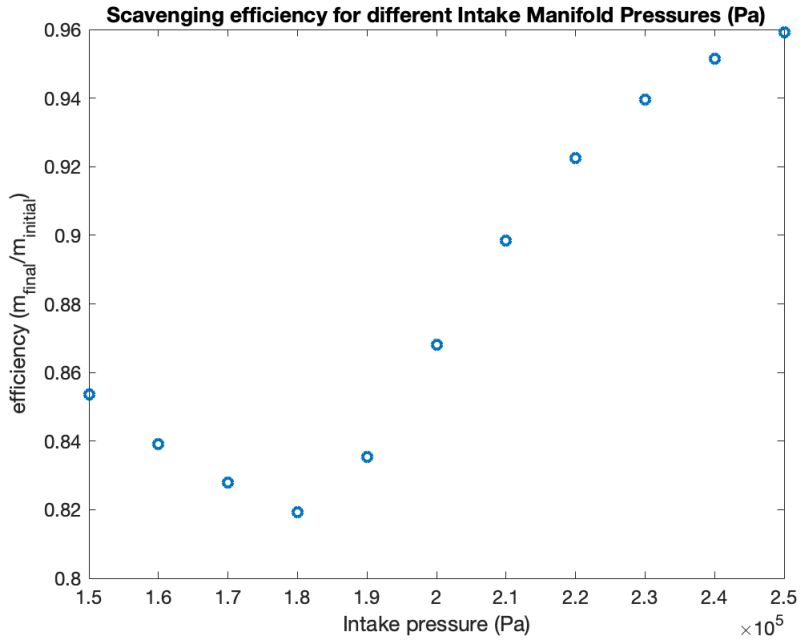

FIG. 7. Scavenging efficiency results for varying intake manifold pressures. Initially, efficiency decreases as intake pressure increases. After intake manifold pressure rises above $1.8 * 10^5$ Pa scavenging increases as intake pressure increases up until reaching an efficiency of 96% at $2.5 * 10^5$ Pa.

B. Varying BDC location

Varying BDC location had a significant impact on scavenging efficiency. We held TDC location constant and varied BDC location by 2 mm increments from 51 mm to 62.5 mm. This changes the amount of time the ports are open, as the distance the cylinder opens beyond the port locations will vary between 1 to 12.5 mm in our runs. Plots of pressure, temperature, and mass profiles, along with a plot of scavenging efficiency are shown in Fig. 8, 9, 10, and 11 below.

For Fig. 8 and 9, the overall shapes of the pressure and temperature curves are similar to those in our trials varying intake manifold pressure. Our plots for BDC location differ most when the ports open. By changing our BDC location, we changed the trajectory of our piston motion, as well as the time at which the ports open and how long they remain open for. In Fig. 8 and 9, we can see this difference in timing of the ports opening as pressure and temperature drop off at a later time when the BDC is closer to the location of the ports

at 50 mm. This result is because the piston is moving much slower when the ports open when the BDC is 51 mm compared to 62.5 mm and takes longer to reach that point.

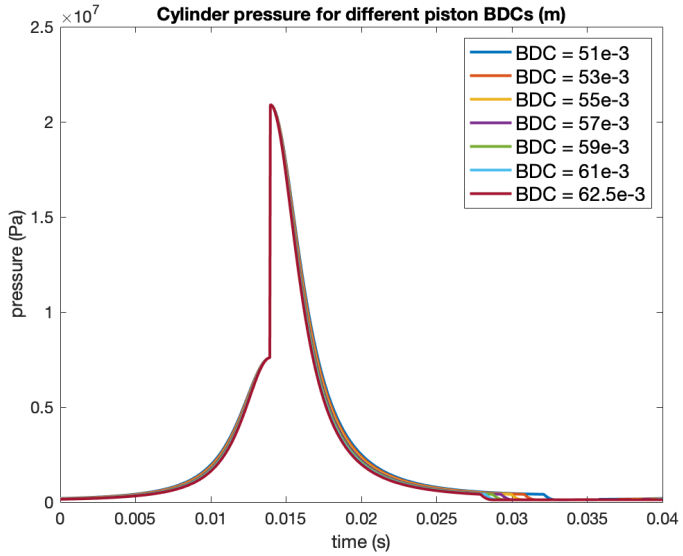

FIG. 8. Cylinder pressure results for varying BDC location. The overall profile of the curve is similar to that of our varying intake manifold pressure trials. The difference in BDC location is most evident when the cylinder pressure drops when the ports open.

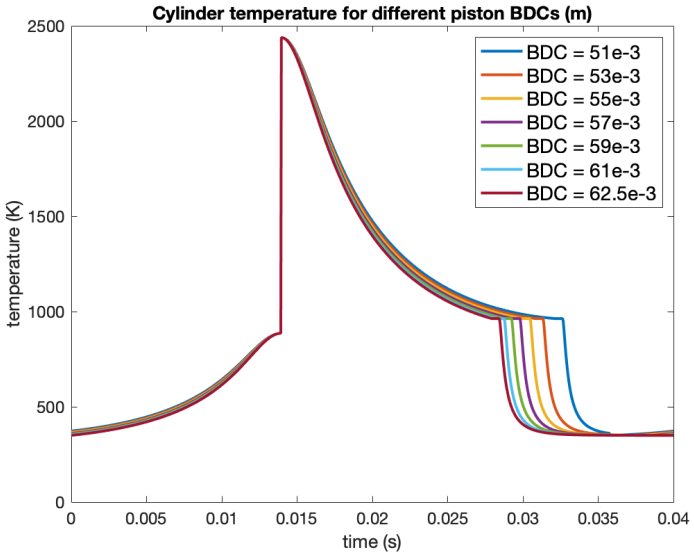

FIG. 9. Cylinder temperature results for varying BDC location. The shape of the curve is similar to those in our varying intake manifold runs. The difference in timing of the ports opening causes the temperature to drop off at later times for smaller BDCs.

Fig. 10 shows results for mass within the cylinder for varying BDC locations. When the BDC location was smaller, the ports opened later and closed sooner, resulting in a shorter time for scavenging to occur. When looking at the curve with a BDC of 51 mm, after the initial drop in mass when the ports open, the ports close again near the curves local maximum. In contrast, when the BDC is 62.5 mm, the mass within the cylinder reaches a maximum larger than the initial mass, before decreasing again as the ports close. For this larger BDC, more fresh-residual gas mixture leaves out of the exhaust port.

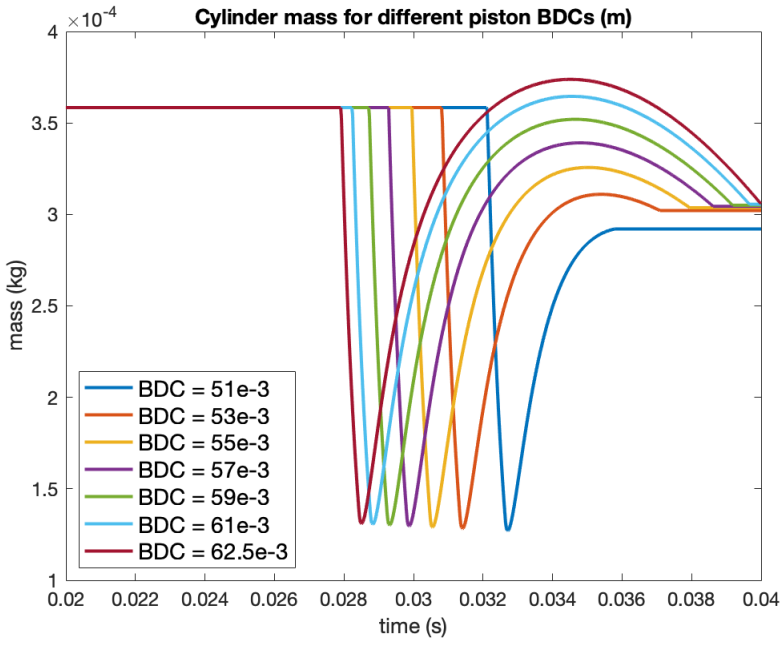

FIG. 10. Cylinder mass results for varying BDC locations. Lower BDC locations correspond with the intake and exhaust ports being open for shorter periods of time. For every run except a BDC of 51 mm, mass within the cylinder reaches a maximum before decreasing as piston volume decreases until the ports close.

Fig. 11 is a plot of scavenging efficiency for different BDC locations. We can see that efficiency increases most between BDCs of 51 and 53 mm. Between 53 and 62.5 mm, efficiency is still increasing, but at a slower rate. From Fig. 10, we see at that at these larger BDCs there is also more fresh charge leaving out of the exhaust port before compressed in the next cycle. Therefore, while scavenging efficiency may be greater when the ports are open for longer, there is also more fresh charge that leaves the cylinder before the engine is able to use it in the next cycle.

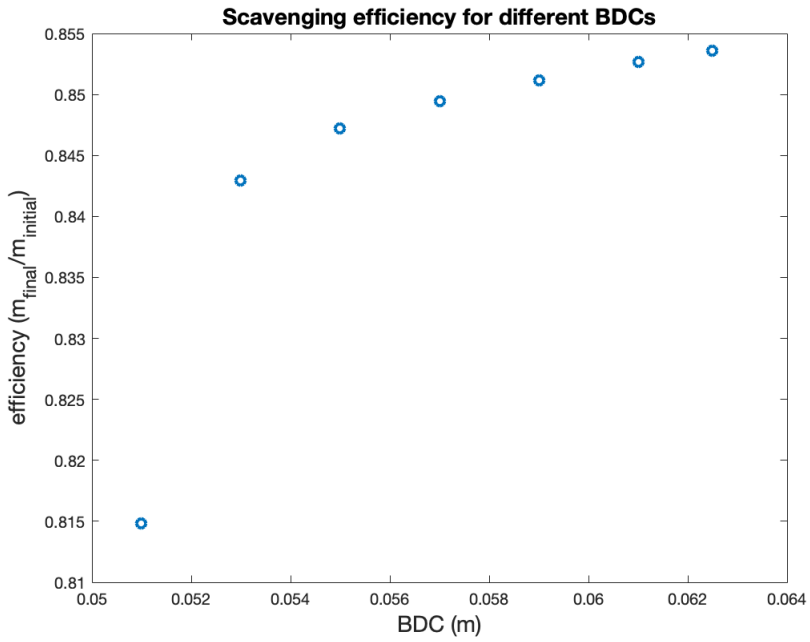

FIG. 11. Scavenging efficiency results for varying BDC location. Scavenging efficiency increased as BDC location increased; however, the largest increase occurs between 51 and 53 mm, with the effect diminishing as BDC increases beyond 53 mm.

V. CONCLUSION

The HFPE at the University of Minnesota offers technology that is able to improve the efficiency of off-road vehicles. We developed a MATLAB Simulink model for scavenging, the process in which exhaust fuel leaves and fresh charge enters a cylinder, for this HFPE. Our model allowed us to vary different initial parameters and track the pressure, temperature, and mass profile of the system. Using our results, we found that high intake manifold pressures and higher BDC locations resulted in a higher scavenging efficiency. These results and findings can be used in the virtual crankshaft controller to improve stable operation of the HFPE.

Future work to be done on this project includes installing more sensors onto the test bed in order to gather more data during testing. With these sensors, we can test the accuracy of the model outlined in this paper and verify its effectiveness. The end goal of this project is to finish development of the virtual crankshaft controller to enable the engine to maintain stable operation under a variety of operating conditions. The engine will then be installed

and tested for use in real world applications.

ACKNOWLEDGMENTS

I would like to thank the Center for Compact and Efficient Fluid Power at the University of Minnesota for providing me with this research experience. I would also like to thank Dr. Zongxuan Sun and Dr. Chen Zhang for their guidance on this project and Ford Motor Company for their generous donation of the hydraulic free-piston engine.

---

[1] Rowland S Benson. A new gas dynamic model for the gas exchange process in two stroke loop and cross scavenged engines. *International Journal of Mechanical Sciences*, 19(12):693–711, 1977.

[2] Ke Li, Ali Sadighi, and Zongxuan Sun. Active motion control of a hydraulic free piston engine. *IEEE/ASME Transactions on Mechatronics*, 19(4):1148–1159, 2013.

[3] GP Merker and M Gerstle. Evaluation on two stroke engines scavenging models. *SAE transactions*, pages 604–627, 1997.

[4] NFPA. What is fluid power? *National Fluid Power Association*, 2017.

[5] Chen Zhang, Ke Li, and Zongxuan Sun. Modeling of piston trajectory-based hcci combustion enabled by a free piston engine. *Applied energy*, 139:313–326, 2015.